

(THRU)  
/ (CODE)  
12 (CATEGORY)

N64-33160  
(ACCESSION NUMBER)

FACILITY FORM 602

54 (PAGES)  
NBA CR 59199  
(NASA CR OR TMX OR AD NUMBER)

Final Report  
for

CYCLOTRON EXCITATION  
OF HYDROMAGNETIC EMISSIONS

(16 Jan. 1964 - 16 Apr. 1964)

Contract No.: NAS5 - 3656

Prepared by  
Lockheed Aircraft Corporation  
(Lockheed Missiles & Space Company)  
3251 Hanover Street  
Palo Alto, California

for  
Goddard Space Flight Center  
Greenbelt, Maryland

OTS PRICE

XEROX \$ 3.00 FS  
MICROFILM \$ .50 ME

## Summary

About  
33160

This report is concerned with the following aspects of sub ELF emissions and related effects:

Part 1: EXPERIMENTAL OBSERVATION OF A NEW TYPE OF SUB ELF EMISSION

From a study of frequency-time characteristics of signals received at four widely separated low-latitude stations, we have ascertained the existence of a low-level sub ELF emission which is almost always present during the night-time hours.

Part 2: ADDITIONAL EVIDENCE FOR THE ATTENUATION OF HYDROMAGNETIC EMISSIONS IN THE IONOSPHERE

A brief analysis of amplitude-time hm-emission data from Palo Alto and Kauai has demonstrated a pronounced ionospheric attenuation effect which verifies previous work at Lockheed on attenuation of hydromagnetic waves in the ionosphere.

Part 3: AN APPROXIMATE UPPER LIMIT TO RING CURRENT DENSITIES

The theoretical maximum trapped particle loading of field lines in the magnetosphere is derived. The result is utilized in Part 4.

Part 4: CYCLOTRON EXCITATION OF HYDROMAGNETIC EMISSIONS

A new model is presented which explains a number of observed hm-emission characteristics.

We believe that the results presented on the following pages more than fulfill the project objectives and may in fact contribute significantly to the understanding of the phenomena of interest.

W. J.

Author

TABLE OF CONTENTS

Part 1

EXPERIMENTAL OBSERVATION OF A NEW TYPE OF SUB ELF EMISSION

Part 2

ADDITIONAL EVIDENCE FOR THE ATTENUATION OF HYDROMAGNETIC EMISSIONS IN THE IONOSPHERE

Part 3

AN APPROXIMATE UPPER LIMIT TO RING CURRENT DENSITIES

Part 4

CYCLOTRON EXCITATION OF HYDROMAGNETIC EMISSIONS

ABSTRACT

I INTRODUCTION

II GENERAL THEORETICAL CONSIDERATIONS

- A. The anomalous Doppler effect
- B. Determination of the radiated frequency
- C. Application of theory to the generation of hm emissions in the magnetosphere
- D. Explanation of rising-frequency fine structure
- E. Latitude dependence of hydromagnetic-emission frequency
- F. Guidance of the hydromagnetic-wave packet

III ENERGY CONSIDERATIONS

- A. Coherency of radiation
- B. Energy radiated by a single proton
- C. Energy received at the earth's surface
- D. Dimensions of the radiating proton stream

## TABLE OF CONTENTS (Continued)

Part 4 (Continued)

- IV. PARTICLE-WAVE MOTION IN THE MAGNETOSPHERE
  - A. The magnetic field of the earth
  - B. Thermal plasma model in the magnetosphere
  - C. Charged particle motion in the magnetosphere
  - D. Alfven wave bounce periods
  - E. Self-consistent model calculations

## ILLUSTRATIONS

<u>Figure</u>		<u>Page</u>
	Part 1	
1	Location of Lockheed Pacific field stations	5
2	Low-level sub ELF emission observed on August 2, 1963	7
3	Low-level sub ELF emission observed on August 3, 1963	9
	Part 2	
1	(Palo Alto)/(Kauai) amplitude ratios as a function of universal time	13
	Part 4	
1	Hydromagnetic emission band showing characteristic fine structure consisting of a series of similar short wave-trains of increasing frequency	21
2	Sample curves for determination of anomalously Doppler shifted proton cyclotron frequency	26
3	Dipole plus uniform magnetic field lines inside a spherical cavity at 10 earth radii	28
4	Proton cyclotron frequency contours for the dipole plus uniform field in the magnetosphere	29
5	Alfven velocity contours for the dipole plus uniform field in the magnetosphere	30
6	Alfven wave bounce periods for the dipole plus uniform field in the magnetosphere	31
7	Self-consistent solutions of the proton cyclotron excitation model for the production of hydromagnetic emissions	39

## TABLES

<u>Table</u>		<u>Page</u>
	Part 4	
1	The hydromagnetic-emission event of November 2, 1961 observed at Palo Alto, California and shown in Figure 1	34
2	Parameters of proton motion in the magnetosphere	44

## Part 1

## EXPERIMENTAL OBSERVATION OF A NEW TYPE OF SUB ELF EMISSION

Lee Tepley and K. D. Amundsen

Research Laboratories  
Lockheed Missiles and Space Company  
Palo Alto, California

The location of the four Lockheed Pacific Ocean stations is shown in Fig. 1. Results are presented elsewhere (Tepley et al., 1963; Tepley, 1964) of properties of hydromagnetic emissions observed simultaneously at the four stations. We are concerned here with the properties of a new type of low level sub ELF emission which seems to almost always be present during nighttime hours. In Figs. 2 and 3 the low level emission is presented in sonagrams from magnetic tape data recorded at the four Pacific stations on two consecutive nights (August 2 and 3, 1963). The sonagrams are characterized by bands of sub ELF energy at all locations except the near equatorial Canton Island station. Thus a pronounced latitude effect is indicated. It is of particular interest that the mid-band frequencies and the number of bands occurring simultaneously may vary greatly at the different stations. It is of equal interest that the mid-band frequencies of all bands at all stations increase slowly but steadily during the night and then decrease relatively abruptly near local sunrise just before the signals fade out.

It is perhaps premature to conclude that the low level signal characteristics shown in Figs. 2 and 3 are characteristic of most nighttime hours. There is however, some indication that this is the case. For example sonagrams from Tongatapu records were obtained for 216 consecutive hours from Aug. 1 through Aug. 9, 1963. During this 9 day period the same general low level signal characteristics presented in Figs. 2 and 3 were observed

every night. In addition, the low level signals are characterized aurally by a howling sound on time compressed magnetic tape. The "howl" seems to be present during most nighttime hours on records from all stations except Canton Island.

The sonagrams of Figs. 1 and 2 are perhaps less striking than those presented in Fig. 1 of Part 4 and elsewhere (Tepley, 1961; Tepley, 1962; Tepley, 1964; Tepley et al., 1964; Tepley and Wentworth, 1962) but this is primarily because they display a signal which is only marginally above the background noise level. The discovery of the existence of this low level signal was an unexpected and surprising result.

The observation of the low level signal indicates that the background signal level near 1 cps is not primarily due to lightning as was previously thought to be the case (Lokken et al., 1963). The signal was not discovered sooner primarily because of its low amplitude (usually less than 1 milligamma - the signal is rarely observed on our helicorder chart records). Also the higher amplitude fine structured hm emissions have previously been of greater interest. It is also possible that the approach of the minimum of the sunspot cycle may lead to improved propagation of these signals through the ionosphere.

The question immediately arises as to whether or not the low-level signals are of the same origin as fine structured hydromagnetic emissions. We cannot presently answer this question but the following comments seem to be in order:

1. The signals do not exhibit a rising-frequency fine-structure characteristic of most hm emissions. However, at times it appears that a continuous transition occurs in which the low-level signals are converted to fine-structured hm emissions. Alternatively, the super-position of fine-structured hm emissions on the low-level signals may be entirely coincidental.
2. The nocturnal appearance of the low-level signals leads to the suggestion that the signals are generated above the ionosphere and are propagated hydromagnetically through the ionosphere suffering severe ionospheric attenuation during the daylight hours (Tepley, 1962; Wentworth, 1963, 1964). If this suggestion



is correct, the signals may be classified as a type of hydromagnetic emission irrespective of the absence of fine structure.

3. In view of the local variation in the mid-band center frequency and the increase in this frequency at all stations throughout the course of the night, it may be suggested that the low level signals originate in the ionosphere, in which case the signal would not be classified as a hydromagnetic emission.

#### ACKNOWLEDGEMENTS

The Lockheed Pacific island stations were set up and operated under contracts AF 19(604)-5906 and AF 19(628)-462 for the Air Force Cambridge Research Laboratories, Office of Aerospace Research. The data presented here was analyzed under contract NAS 5-3656 for the National Aeronautics and Space Administration. We wish to acknowledge the following individuals who were responsible for maintaining the stations in continuous operation: R. P. Gerrish, D. R. Hillendahl, K. G. Lambert, H. V. Prentiss, J. Reichelmann, and R. C. Wentworth.

Fig. 1. Location of the Lockheed Pacific Stations

Geographic coordinates are indicated at the left of the above map. Geomagnetic coordinates are indicated at the right. The coordinates of the stations are as follows:

	Geographic Latitude	Geographic Longitude	Geomagnetic Latitude	Geomagnetic Longitude
Canton Island (Phoenix Group)	02°46'S	171°43'W	05.1°S	258.0°E
Kauai, Hawaii	22°09'N	159°18'W	21.7°N	265.6°E
Palo Alto, California	37°26'N	122°10'W	43.5°N	299.0°E
Tongatapu, (Tonga Group)	21°14'S	175°08'W	24.0°S	258.5°E

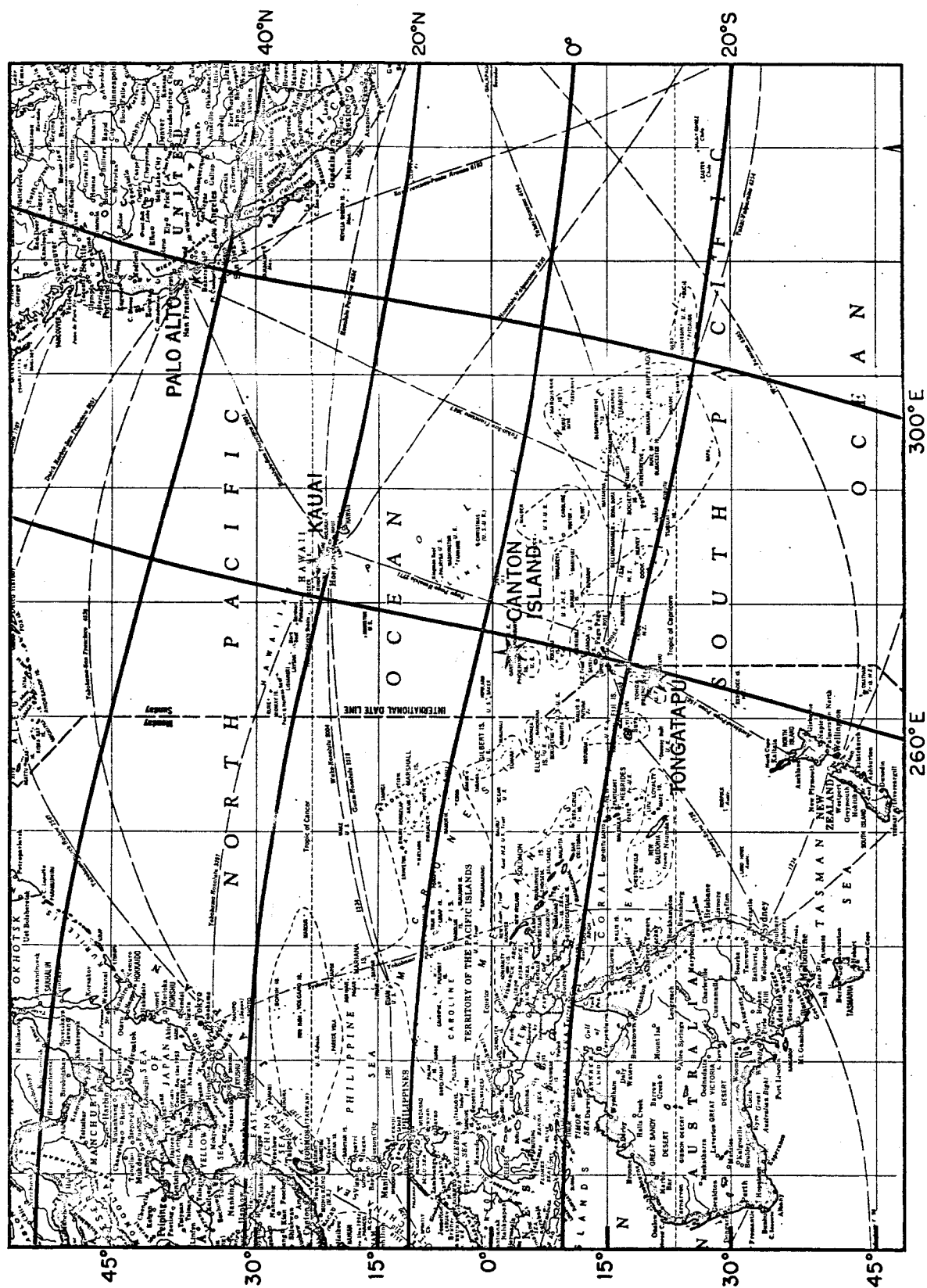


Fig. 2. Low-Level Sub ELF Emissions Observed on 2 August 1963

Low-level emissions are observed at Palo Alto, Kauai, and Tongatapu. Note the different appearance of the bands at the different stations. In particular note that at Kauai, three bands are observed simultaneously in the interval 0800-1300. Note also that the mid-frequencies of all bands increase slowly throughout the night and then decrease relatively rapidly near sunrise (the effect is not observed at Palo Alto where the signal fades out in the middle of the night). In the time interval 1000-1900, signals are observed simultaneously at all stations at frequencies below 0.1 cps. These represent long period micropulsations. The series of faint equally spaced horizontal narrow bands which are observed all across the sonagrams at frequencies below 0.2 cps result from instrumental noise.

PALO ALTO

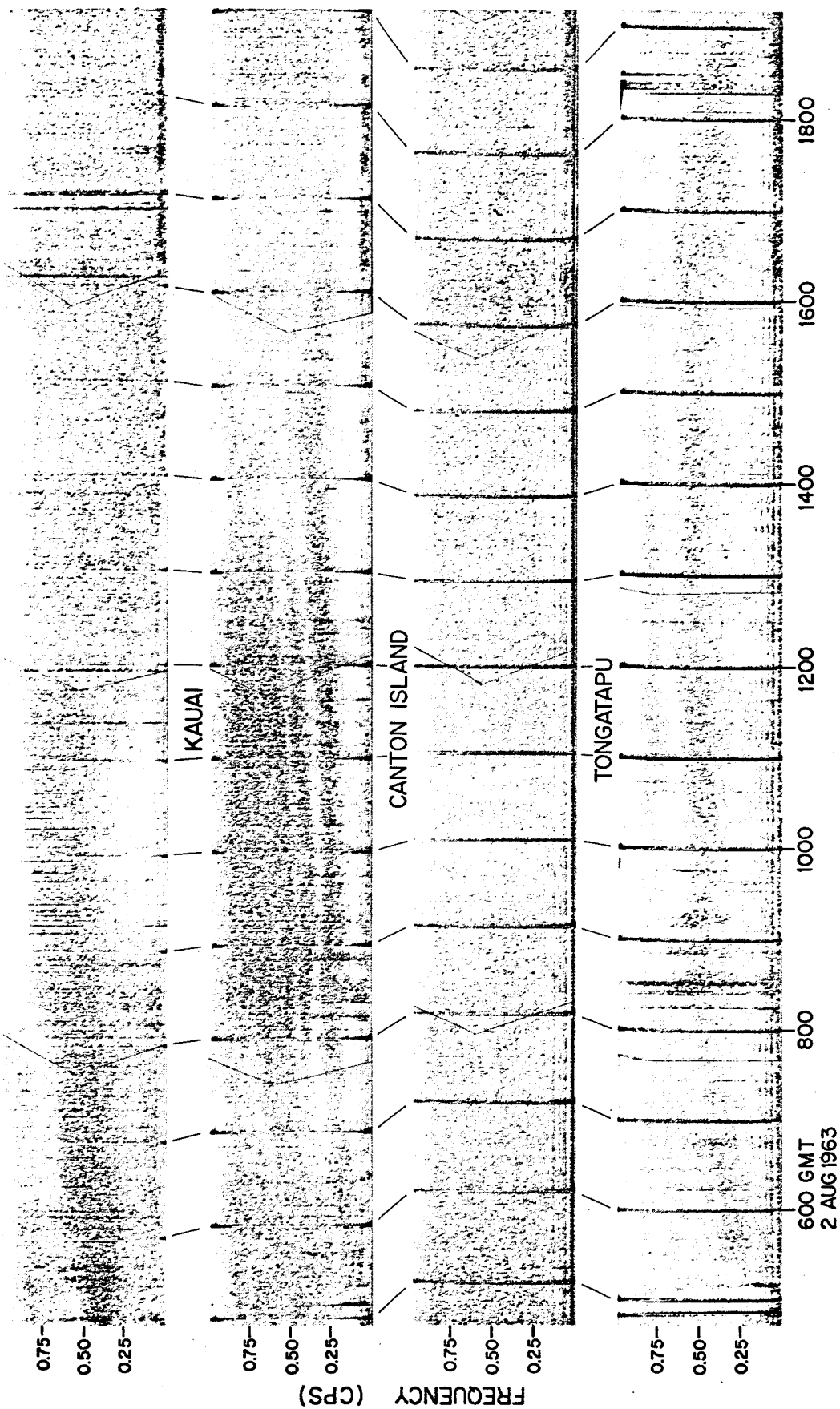
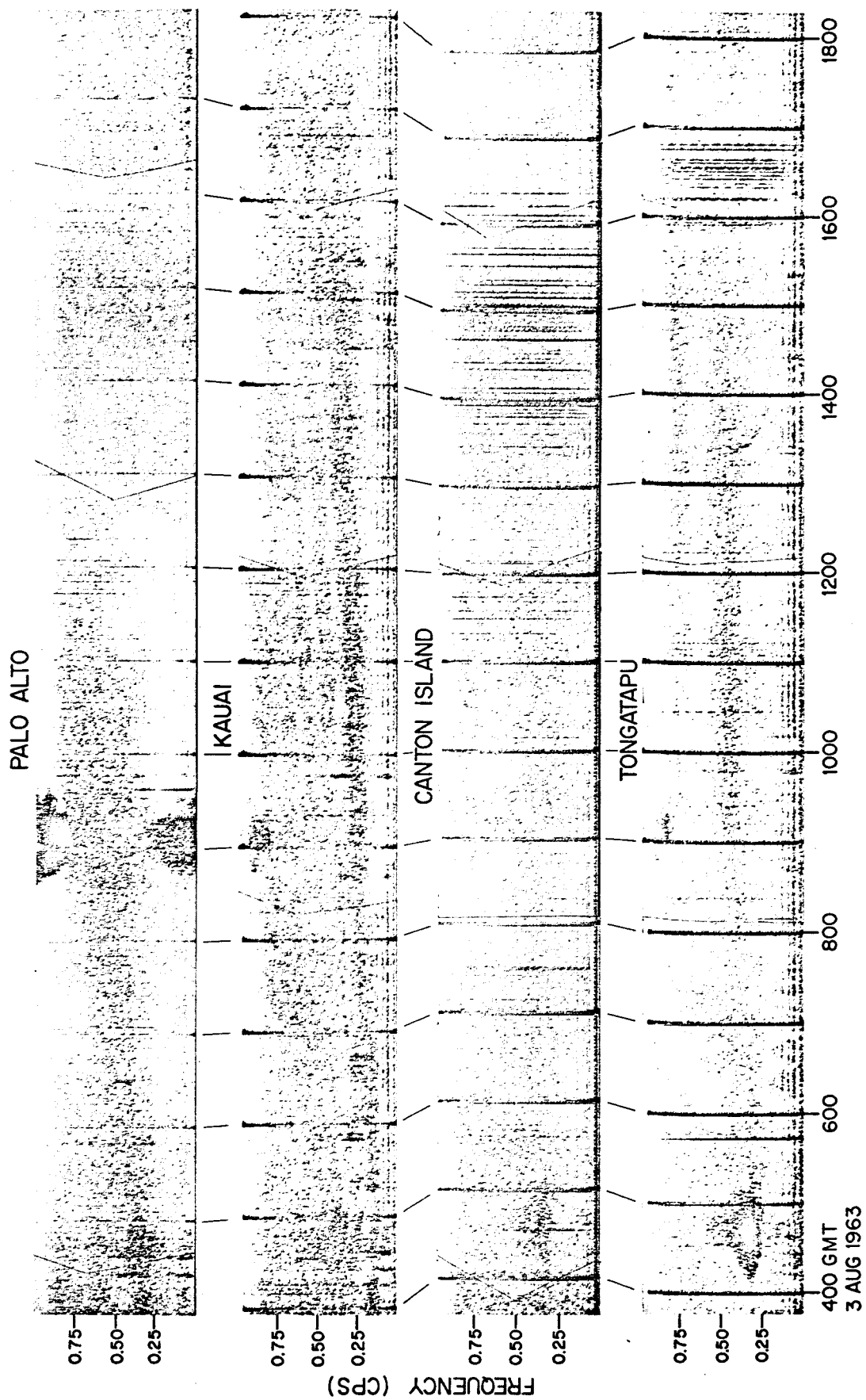
600 GMT  
2 AUG 1963

Fig. 3. Low-Level Sub ELF Emissions Observed on 3 August 1963

The low-level emissions are similar to those illustrated in the previous figure, but are somewhat less intense at Palo Alto than at Kauai. In the interval 0415-0515 an intense hm emission is observed simultaneously at all stations. The signal is somewhat different in appearance than those shown on sonagrams presented elsewhere because of the large tape speed-up factor utilized here (about 8000). Note that at Palo Alto, the hm emission is super-imposed on the low-level emission. A second hm emission is observed in the time interval 0840-0935. The signal is intense at Palo Alto, faint at Kauai and Tongatapu and indiscernible at Canton Island. The signal at Palo Alto directly beneath the second emission is the frequency range 0-0.25 cps is produced by overloading by the second emission of the playback instrumentation. In this case overloading resulted because of the high amplification necessary to bring out the low-level emissions.



# REFERENCES

- Lokken, J. E., J. A. Shand, and C. S. Wright, Some characteristics of electromagnetic background signals in the vicinity of one cycle per second, J. Geophys. Res. 68, 789-794, 1963.
- Tepley, L. R., Observations of hydromagnetic emissions, J. Geophys. Res. 66, 1651-1658, 1961.
- Tepley, L. R., Structure and attenuation of hydromagnetic emissions, Vol. 1, Sci. Rept. 1 (contract AF 19(604)-5906, Electronic Research Directorate, Air Research and Development Command), April 6, 1962.
- Tepley, L. R., Low latitude observations of fine-structured hydromagnetic emissions, to be published in J. Geophys. Res. 69, June, 1964.
- Tepley, L. R. and R. C. Wentworth, Hydromagnetic emissions, x-ray bursts, and electron bunches, Part I: experimental results, J. Geophys. Res. 67, 3317-3333, 1962.
- Tepley, L. R., R. C. Wentworth, and K. D. Amundsen, Sub ELF geomagnetic fluctuations, Vol. I: frequency-time characteristics of hydromagnetic emissions, Final Report, contract AF 19(628)-462 for Air Force Cambridge Research Laboratory, Office of Aerospace Research, 26 December, 1963.
- Wentworth, R. C., Sub ELF geomagnetic fluctuations, Vol. II: statistical studies of hydromagnetic emissions, Final Report, contract AF 19(628)-462 for Air Force Cambridge Research Laboratory, Office of Aerospace Research, 26 December 1963.
- Wentworth, R. C., Evidence for maximum production of hydromagnetic emissions above the afternoon hemisphere of the earth, Part II: analysis of statistical studies, to be published in J. Geophys. Res. 69, July 1, 1964.



Part 2  
ADDITIONAL EVIDENCE FOR THE ATTENUATION  
OF HYDROMAGNETIC EMISSIONS IN THE IONOSPHERE

R. C. Wentworth and Lee Tepley

Research Laboratories  
Lockheed Missiles and Space Company  
Palo Alto, California

It has been recognized for some time that hydromagnetic waves in the frequency interval around 1 cps can be severely attenuated in the daytime ionosphere (Dessler, 1959; Francis and Karplus, 1960; Karplus et al., 1962). Tepley (1962) first demonstrated that this property could be used to explain the diurnal variation in amplitudes of hm emissions observed at middle latitudes. More recently Wentworth (1963, 1964) demonstrated that the same hydromagnetic-wave attenuation characteristic could be applied to explain the difference in diurnal variation of emissions observed at middle and high latitudes. In this note additional evidence is presented which demonstrates the influence of ionospheric attenuation on signals observed simultaneously at middle and low latitude stations.

Recently, a preliminary analysis was carried out on amplitudes of hm emissions observed simultaneously at Palo Alto, California, and Kauai, Hawaii, from September 15, 1963 through November 3, 1963. The resulting amplitude ratios of Palo Alto to Kauai were plotted as a function of universal time, and a striking pattern emerged which lends strong additional support to the hypothesis of heavy daytime hydromagnetic-wave attenuation in the ionosphere at middle and low latitudes.

The results of this analysis are plotted in Fig. 1. It can be seen that the amplitude ratio is exceptionally high during the time of day which

is after sunset at Palo Alto, but before sunset at Kauai. At the other end of the scale, those events which occurred after sunrise at Palo Alto and before sunrise at Kauai exhibit amplitude ratios of somewhat less than one.

It appears that two main factors are influencing the relative amplitudes of emissions observed simultaneously at Palo Alto and Kauai. First, heavy attenuation is occurring above Kauai before local sunset relative to the post sunset conditions above Palo Alto at the same time. Likewise, heavy attenuation is occurring above Palo Alto after local sunrise relative to pre-sunrise conditions above Kauai at the same universal time. Second, a pronounced latitude effect exists with amplitudes at Palo Alto being roughly six times those at Kauai for comparable ionospheric conditions.

#### ACKNOWLEDGEMENTS

The Palo Alto and Kauai stations were set up and operated under contracts AF 19(604)-5906 and AF 19(628)-462 for the Air Force Cambridge Research Laboratories, Office of Aerospace Research. The data presented here was analyzed under contract NAS 5-3656 for the National Aeronautics and Space Administration. We wish to acknowledge the following individuals for their work in setting up and operating the stations: K. D. Amundsen, D. R. Hillendahl, K. G. Lambert and H. V. Prentiss. We also wish to acknowledge K. D. Amundsen for his assistance in data reduction.

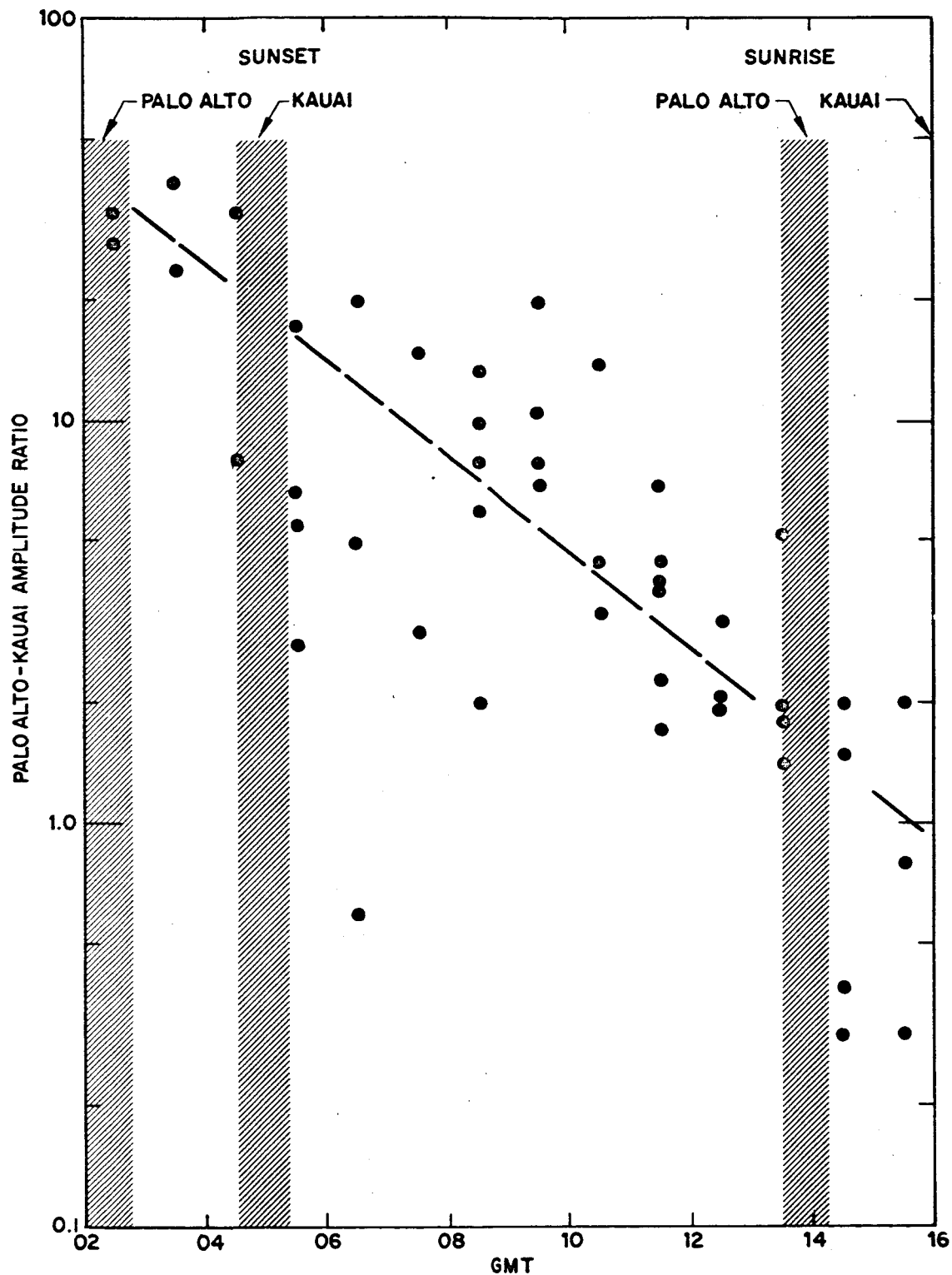


Figure 1. (Palo Alto)/(Kauai) amplitude ratios as a function of universal time. The ratios vary from 30 before sunset at Kauai to about 0.8 after sunrise at Palo Alto, with an average of about 6 around midnight.

# REFERENCES

- Dessler, A. J., Ionospheric heating by hydromagnetic waves, J. Geophys. Res. 64, 397-401, 1959.
- Francis, W. D. and R. Karplus, Hydromagnetic waves in the ionosphere, J. Geophys. Res. 65, 3593-3600, 1960.
- Karplus, R., W. E. Francis, and A. J. Dragt, The attenuation of hydromagnetic waves in the ionosphere, Planetary and Space Science, Pergamon Press, Vol. 9, pp. 771-785, 1962.
- Tepley, L. R., Structure and attenuation of hydromagnetic emissions, Vol. 1, Sci. Rept. 1 (contract AF 19(604)-5906, Electronic Research Directorate, Air Research and Development Command), April 6, 1962.
- Wentworth, R. C., Sub ELF geomagnetic fluctuations, Vol. II: statistical studies of hydromagnetic emissions, Final Report, contract AF 19(628)-462 for Air Force Cambridge Research Laboratory, Office of Aerospace Research, 26 December 1963.
- Wentworth, R. C., Evidence for maximum production of hydromagnetic emissions above the afternoon hemisphere of the earth, Part II: analysis of statistical studies, to be published in J. Geophys. Res. 69, July 1, 1964.

Part 3  
AN APPROXIMATE UPPER LIMIT  
TO RING CURRENT DENSITIES

R. C. Wentworth

Research Laboratory  
Lockheed Missiles and Space Company  
Palo Alto, California

It was first pointed out by Beard (1962) that the maximum perpendicular energy density of trapped ring current particles which could be contained by the earth's magnetic field in the magnetosphere was approximately one quarter of the unperturbed magnetic field energy density. It is the purpose of the present note to re-derive this result in order to stress a parallel development to Beard's analysis, namely that the minimum perturbation field resulting from trapped ring current particles is one-half of the unperturbed value.

Beard (1962) showed that the perturbation field due to the trapped ring current particles is predominantly due to the diamagnetic effect of the trapped particles in the vicinity of the test point. The magnetic moment of a single spiraling particle, defined as the current generated by its gyration times the area enclosed, is given by (see e.g. Apel et al., 1963)

$$\mu = \frac{e}{c} \frac{\pi \rho^2}{t} = \frac{E_{\perp}}{B}$$

and the magnetic moment per unit volume in the vicinity of the test point is

$$M = N_0 \mu = N_0 E_{\perp} / B$$

It is useful to note that the magnetic field in the interior of a uniformly magnetized sphere of magnetization  $M$  per unit volume is

$$\Delta B_s = (8\pi/3)M$$

while the magnetic field in the interior of a uniformly magnetized semi-infinite cylinder of magnetization  $M$  per unit volume is

$$\Delta B_c = 8\pi M$$

Therefore, let us take as an approximation to the magnetic field produced by the trapped ring current particles in the vicinity of the test point,

$$\Delta B_M = (8\pi/\xi)M = \frac{8\pi}{\xi} \frac{N_o E_{\perp}}{B}$$

where

$$1 \leq \xi \leq 3$$

The magnetic field at the test point is then given by

$$B = B_o - \frac{8\pi}{\xi} \frac{N_o E_{\perp}}{B} \quad (1)$$

where  $B_o$  is the unperturbed field in the absence of ring current particles at the test point. Solving for  $B$ , we have

$$B = \frac{B_o}{2} \cdot \left[ 1 + \left( 1 - \frac{4\beta}{\xi} \right)^{1/2} \right] \quad (2)$$

where

$$\beta = \frac{N_o E_{\perp}}{B_o^2 / 8\pi}, \quad 1 \leq \xi \leq 3$$

Equation (2) is equivalent to the final result of Beard (1962).

Results. Equation (2) implies that the minimum perturbation field which can be produced by trapped ring current particles is given by

$$B_{\min} = B_0/2 \quad (3)$$

where  $B_0$  is the unperturbed field at the test point in the absence of trapped particles. In addition, the maximum trapped ring current density which can be sustained in the vicinity of the test point is given by

$$\beta_{\max} = \frac{(N_0 E_1)_{\max}}{(B_0^2/8\pi)} = \frac{\xi}{4} \quad (4)$$

where

$$1 \leq \xi \leq 3$$

As mentioned previously, this result was obtained by Beard (1962) who assumed throughout that  $\xi$  was equal to 1. We note that in this case the maximum trapped particle energy density,  $N_0 E_1$ , is equal to the minimum perturbation field energy density,  $B^2/8\pi$ .

Critical Discussion. We conclude that the minimum perturbation field is one-half of the unperturbed field, and the maximum trapped particle energy density is one-fourth of the unperturbed magnetic field energy density. As mentioned above, these conditions lead to equality between the trapped particle energy density and the perturbed magnetic field energy density. If more particles are injected the perturbation field cannot contain them and the excess particles will be blown out the sides of the flux tube until conditions (3) and (4) are everywhere fulfilled.

#### ACKNOWLEDGEMENTS

The author wishes to acknowledge stimulating discussions and helpful suggestions from D. B. Beard, A. J. Dessler, and E. J. Smith. This research was done under contract NAS 5-3656 for the National Aeronautics and Space Administration.

REFERENCES

Beard, D. B., Self-consistent calculation of the ring current, J. Geophys.  
Res. 67, 3615-3616, 1962.



## Part 4

## CYCLOTRON EXCITATION OF HYDROMAGNETIC EMISSIONS

Lee Tepley and R. C. Wentworth

Research Laboratories

Lockheed Missiles and Space Company

Palo Alto, California

ABSTRACT

A new model for the production of hydromagnetic emissions is presented. Hydromagnetic emissions are typically characterized by two frequencies; the emission frequency on the order of 0.5-3.0 cps, and the repetition frequency of the fine-structured elements on the order of 0.2-1.0 cycles per minute (periods of 1 to 5 minutes). The model explains these two characteristic frequencies as being determined by two natural parameters of the motion of proton streams in the magnetosphere. The emission frequency is the anomalously Doppler shifted proton cyclotron frequency in the vicinity of the equatorial plane, and the period of the fine-structured elements, observed experimentally to be received alternately in the two hemispheres, is determined by the bounce period of the proton stream as it mirrors successively above the northern and southern hemispheres. The model explains the rising-frequency emission fine structure in terms of velocity spread in the proton stream, and predicts the experimentally observed latitude dependence of hm emission frequency.

## I. INTRODUCTION

Recent experimental observations (Tepley, 1964; Tepley et al, 1964) have conclusively demonstrated that the regularly spaced fine-structured elements which constitute most hm emissions (Figure 1) are observed simultaneously at stations in the same hemisphere, but are alternately spaced ( $180^\circ$ ) out of phase) in emissions observed simultaneously on opposite sides of the equator. Hence, hm-emission energy is received periodically and alternately in the northern and southern hemispheres. This result is suggestive of a slow energy bounce between hemispheres (bounce times are typically on the order of 1 to 4 minutes). Jacobs and Watanabe (1963) have interpreted this result in terms of a model involving geomagnetically trapped proton bunches of solar-wind energies bouncing between hemispheres and generating hm emissions in the lower exosphere by means of a hydromagnetic resonance effect. However, the theoretically predicted latitude dependence of the hm-emission frequency, associated with the hydromagnetic resonance, is in disagreement with experimental observations (Tepley, 1964; Tepley et al, 1964; Wentworth, 1964a,b). Hence their model is inadequate.

More recently Jacobs and Watanabe (1964) have presented an alternative model in which hm emissions are generated by hydromagnetic wave packets bouncing between hemispheres. The wave packets propagate in the Alfvén mode and are guided by the geomagnetic field. However, the authors have not quantitatively considered the important but probably very difficult problem of the extent to which the waves are guided. Unless guidance is almost perfect, an exponential decay should be observed in the intensities of successive fine-structured elements which represent successive arrivals of the hydromagnetic wave packets. This is usually not observed experimentally. Instead the emission band generally increases slowly in intensity (typically over a 10-15 minute period) and then decreases in intensity at about the same rate. It thus appears that energy is being continuously supplied to the wave packet, so that extremely close guidance of the packet by the magnetic field is not necessarily required in order to sustain the packet for a large number of bounces.

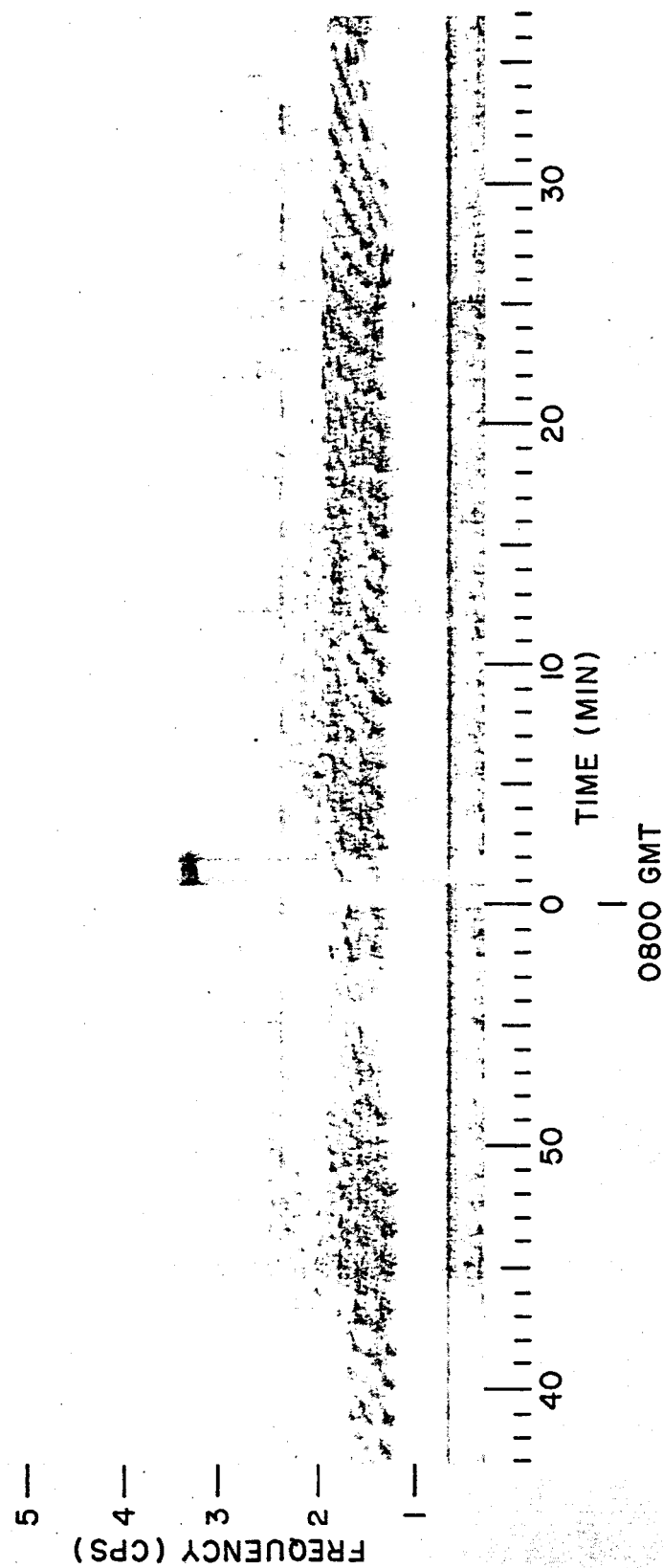


Fig. 1 Hydromagnetic Emission Band (Characteristic fine structure consisting of a series of similar short wavetrains of increasing frequency)

In this paper we again consider concepts similar to those utilized by Jacobs and Watanabe. The concept of bouncing proton bunches, however, while easy to visualize, seems difficult to justify on physical grounds. It is perhaps more realistic to consider the protons as moving in streams of unspecified dimensions along geomagnetic field lines. We consider proton streams and hydromagnetic-wave packets (propagating in the Alfvén mode) characterized by approximately the same bounce time between opposite hemispheres. We also specify that the streams and wave packets move in the same direction and that they cross the equatorial plane at about the same time. We suggest that the wave packets are initially generated by the proton streams in the vicinity of the equatorial plane. Thus in each successive crossing of the equatorial plane, the stream imparts additional energy to the wave packet to compensate for losses due to imperfect guidance by the magnetic field. In this way the energy of the packet builds up until the stream and packet drift out of phase.

The proposed mechanism might at first appear to resemble the traveling wave amplification mechanism proposed for the generation of VLF emissions (Gallet, 1959; Gallet and Helliwell, 1959). However the model does not actually utilize traveling wave amplification in the usual sense wherein the interaction between particles and waves occurs when both move at about the same velocity. Instead the energy transfer occurs when the stream velocity exceeds the wave velocity by a significant factor. In this preliminary paper we do not actually consider the particle-wave interaction but only the radiation of energy by protons in the stream in appropriate time-phase to reinforce the wave packet generated by the stream at an earlier time.

There is some evidence that a significant percentage of alpha particles is present in the solar wind. Thus alpha particles of solar wind energies might conceivably be trapped in the geomagnetic field and would also radiate energy in the form of hydromagnetic waves, but at lower frequencies than those calculated in this paper for radiation from proton streams; we are concerned here, however, only with proton radiation.

In concluding our introductory remarks we comment that, in contrast to the first proton bunch model of Jacobs and Watanabe, the present model pre-

dicts the observed latitude dependence of hm-emission frequency. The model also leads to an alternative explanation of the rising-frequency emission fine structure. We also note that although the present model does not require extremely close guidance of the hydromagnetic wave packets, a mechanism for close guidance is inherent in those calculations which utilize loaded magnetic field lines (as discussed in Part 3 of this report) and a plasma density "knee" in the magnetosphere.

## II. GENERAL THEORETICAL CONSIDERATIONS

We postulate that the hydromagnetic wave packet is propagated along a geomagnetic field line in the Alfvén mode and a large fraction of the wave energy is reflected near the end of the line. Thus the wave packet "bounces" between hemispheres. We consider Alfvén mode propagation only since the other hydromagnetic wave mode (the so-called magneto-sonic wave) is not significantly guided by the geomagnetic field, and recent experimental observations (Tepley, 1964; Tepley et al, 1964) demonstrate that a significant amount of guidance occurs. However, we do not require almost perfect guidance nor do we require almost complete reflection near the end of the field line, since the energy of the wave packet is reinforced on every bounce near the equatorial plane by cyclotron radiation from proton streams which cross the equatorial plane coincidentally with the wave packet.

A. The anomalous Doppler effect. An association between the hm-emission frequency and the proton cyclotron frequency was suggested by one of the authors in earlier papers (Tepley, 1961a,b). The suggestion is subject to the apparent difficulties that the Alfvén wave does not propagate at (or above) the proton cyclotron frequency, and that strong cyclotron (collisionless) absorption and thermal absorption occur when the wave frequency is near the proton cyclotron frequency. These difficulties are resolved when the radiating stream has a substantial velocity component along the magnetic field, in which case the frequency of the radiated wave is Doppler shifted away from the proton cyclotron frequency. In this paper we consider cyclotron radiation from proton streams moving "faster than light" - that is, moving with a velocity along the magnetic field which exceeds the

phase velocity of the hydromagnetic wave in the magnetosphere. In this case the Doppler shift is "anomalous", that is, the frequency of radiation in the forward direction is shifted downward. The equation for the anomalous Doppler effect may be written as follows:

$$\frac{\omega}{\omega_c} = \left( \frac{v_{||}}{V_a} \cdot n \cdot \cos \theta - 1 \right)^{-1} \quad (1)$$

where  $\omega_c$  is the proton cyclotron frequency,  $\omega$  is the Doppler shifted hydromagnetic wave frequency,  $v_{||}$  is the component of proton velocity along the magnetic field,  $V_a$  is the Alfvén velocity,  $\theta$  is the angle between the propagation vector of the wave and the magnetic field, and  $n = V_a/V_\phi$  is the index of refraction of the medium. ( $V_\phi$  is the phase velocity of the hydromagnetic wave propagating in the Alfvén mode.)

The possible importance of anomalously Doppler shifted cyclotron radiation for the production of geomagnetic micropulsations was first pointed out in an excellent paper by M. A. Ginzburg (1962). The model presented in this paper is essentially an application of the basic concepts presented by Ginzburg.

B. Determination of the radiated frequency. For propagation of an Alfvén wave in a cold plasma, the index of refraction of the plasma is

$$n = \frac{1 + \cos^2 \theta + \sqrt{\sin^2 \theta + 4x^2 \cos^2 \theta}}{2 \cos^2 \theta (1 - x^2)} \quad (2)$$

where  $x = \omega/\omega_c$  is the dimensionless hydromagnetic-wave frequency. The above equation is valid for all values of  $\theta$  except those very near  $90^\circ$ .

By combining Equations (1) and (2) we obtain the following expression:

$$\left( \frac{v_{||}}{V_a} \right)^2 = \left( 1 + \frac{1}{x} \right)^2 \cdot \frac{2(1 - x^2)}{1 + \cos^2 \theta + \sqrt{\sin^2 \theta + 4x^2 \cos^2 \theta}} \quad (3)$$

Thus for any given value of  $v_{||}/V_a$  and  $\theta$  the radiated frequency is uniquely determined. Equation (3) is strictly valid for determination of the frequency of the radiation from a single particle, since if we were to consider

a stream of radiating particles, the expression for the index of refraction of the plasma would be modified.

In Figure 2, a plot is presented of  $v_{||}/V_a$  versus  $\theta$  for four values of the parameter  $x$ . The fact that the series of curves are in the form of almost horizontal lines shows that almost the same frequency is radiated in any forward direction (a pronounced angular dependence of radiated frequency is obtained when the same procedure is carried out for the magneto-sonic wave). Hence, to a close approximation, the radiated frequency resulting from the anomalous Doppler shift of the Alfvén wave at any angle  $\theta$  is the same as that observed at  $\theta = 0$  and given by

$$\frac{v_{||}}{V_a} = \left(1 + \frac{1}{x}\right) \sqrt{1-x} \quad (4)$$

A curve for the above equation is presented in Figure 7. It may be seen from the curve that for  $x \leq 0.6$ , the equation simplifies further to

$$\frac{v_{||}}{V_a} \approx \frac{1}{x} = \frac{\omega_c}{\omega} \quad (5)$$

C. Application of theory to the generation of hm emissions in the magnetosphere. In order to apply the above concepts we require a knowledge of the plasma density and magnetic field strength in the magnetosphere as a function of position in space. Both of these quantities are time varying and few precise measurements have been made. For the plasma density we present calculations based on the following models:

(1) A model of a "normal" magnetosphere based on whistler data obtained from Liemohn and Scarf (1964).

(2) A model of a magnetosphere characterized by a "knee" (Carpenter, 1963). In our case we assume that beyond the knee the plasma density has been reduced from its normal value by a factor of 9.

For the magnetic field strength, we also present calculations based on two models as follows:

(1) As a first approximation to the solar wind cavity on the daylight side of the earth, we consider a dipole field confined to the interior of a

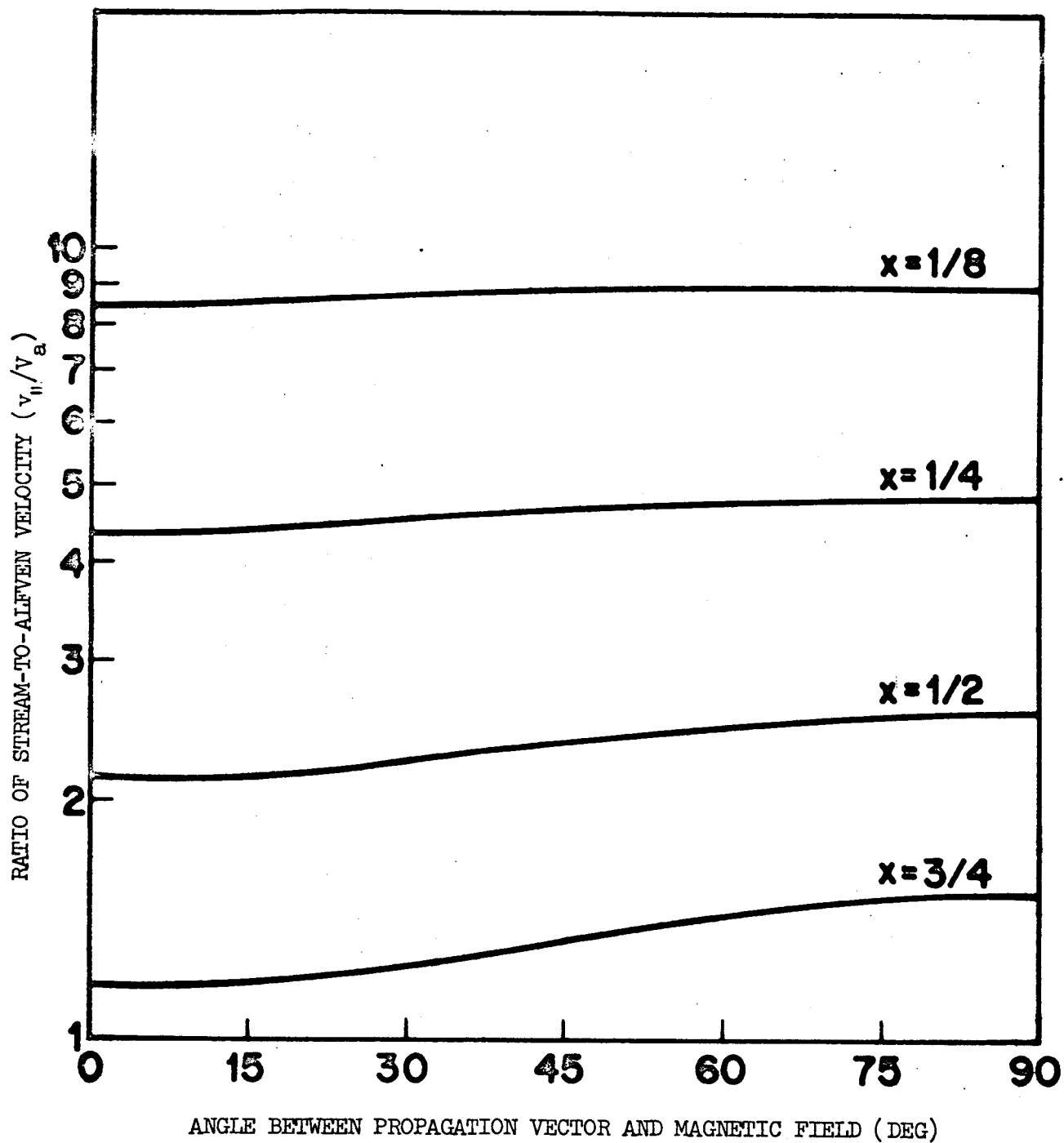


Fig. 2 Sample curves for determination of anomalously Doppler shifted cyclotron frequency



sphere (Wentworth and Tepley, 1962; Figure 3).

(2) As a second approximation, we include the effects of a reduction or "loading" of the magnetic field in certain regions due to the presence of additional protons of solar wind energy such as those which are thought to constitute "ring currents" (loading of the magnetosphere has been discussed in Part 3 of this report).

We consider the solar wind cavity only on the daylight side of the earth because of the relative ease of calculation of magnetic field strength, and also because hm emissions are thought to be generated mostly on the daylight side, even though they are observed most frequently at night at middle and low latitudes (Wentworth, 1964a,b). From the various models for plasma density and magnetic field strength we are able to calculate proton cyclotron frequencies (Figure 4) and Alfvén velocities under various conditions (Figure 5). By integration of the Alfvén velocity along a magnetic field line, we calculate the bounce period of the Alfvén wave packet as a function of latitude (Figure 6). This calculation is not strictly applicable to the present model since the packet bounce time is actually determined by the hydromagnetic-wave group velocity rather than the Alfvén velocity. The two velocities almost coincide when the wave frequency is much less than the proton cyclotron frequency, a condition which is fulfilled over a large part of the packet trajectory. However, a significant deviation can occur in the vicinity of the equatorial plane if the wave frequency approaches the local proton cyclotron frequency, a condition which can occur when the frequency shift due to the anomalous Doppler effect is small. A more exact calculation of wave packet bounce time similar to that made by Jacobs and Watanabe (1964) is contemplated at a later date. It is felt, however, that the approximate calculation presented here is adequate to indicate the "reasonableness" of the present model.

The proton stream bounce time is specified by the requirement that it coincide with the wave packet bounce time calculated in the manner just described. We restrict our discussion to protons moving in orbits characterized by a relatively small pitch angle, in which case the stream bounce time is almost independent of pitch angle. Since the bounce time is specified,

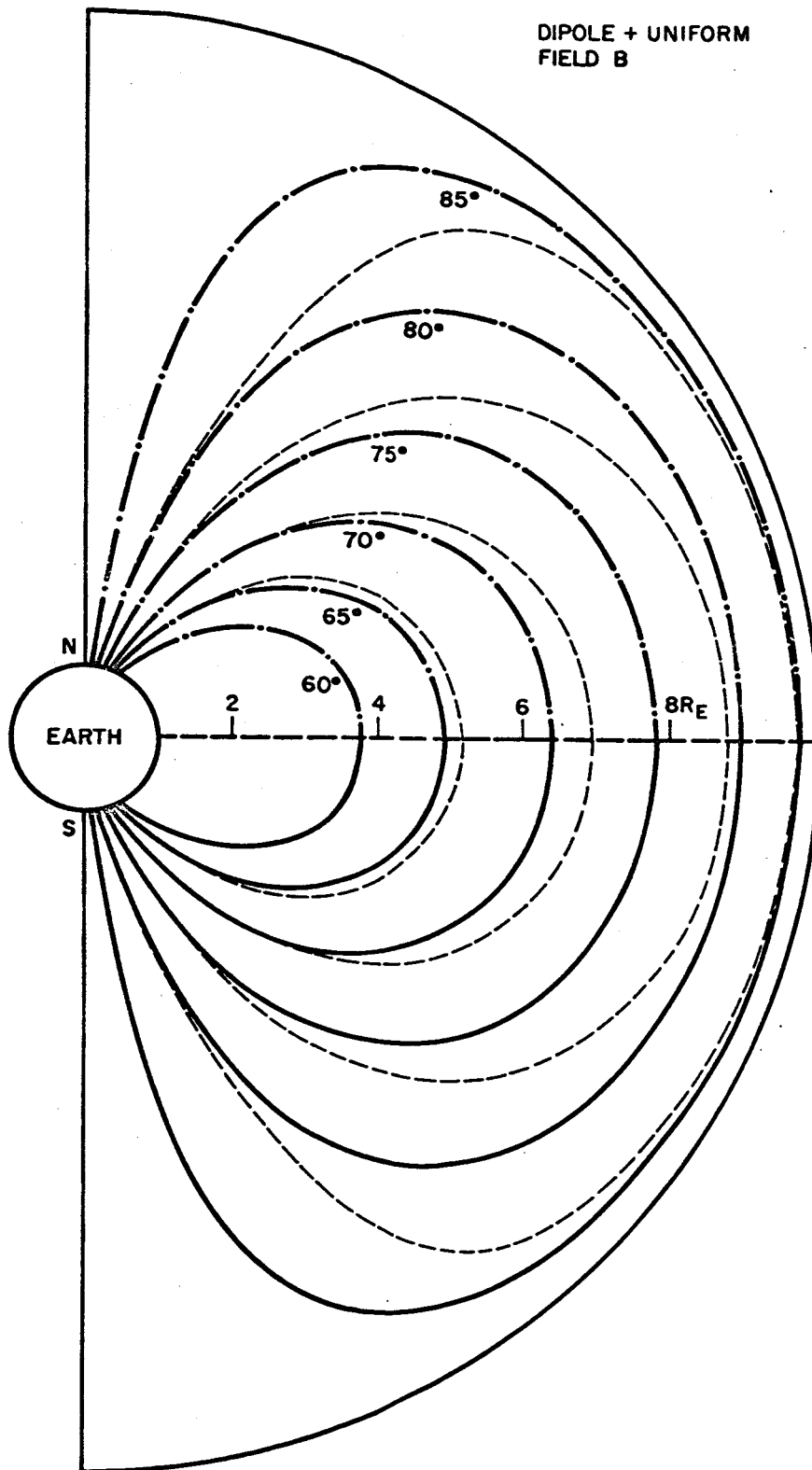


Figure 3. Dipole plus uniform magnetic field lines inside a spherical cavity at 10 earth radii. For comparison the deformation of the geomagnetic field by the solar wind computed by Mead (1964) is indicated by the dashed lines.

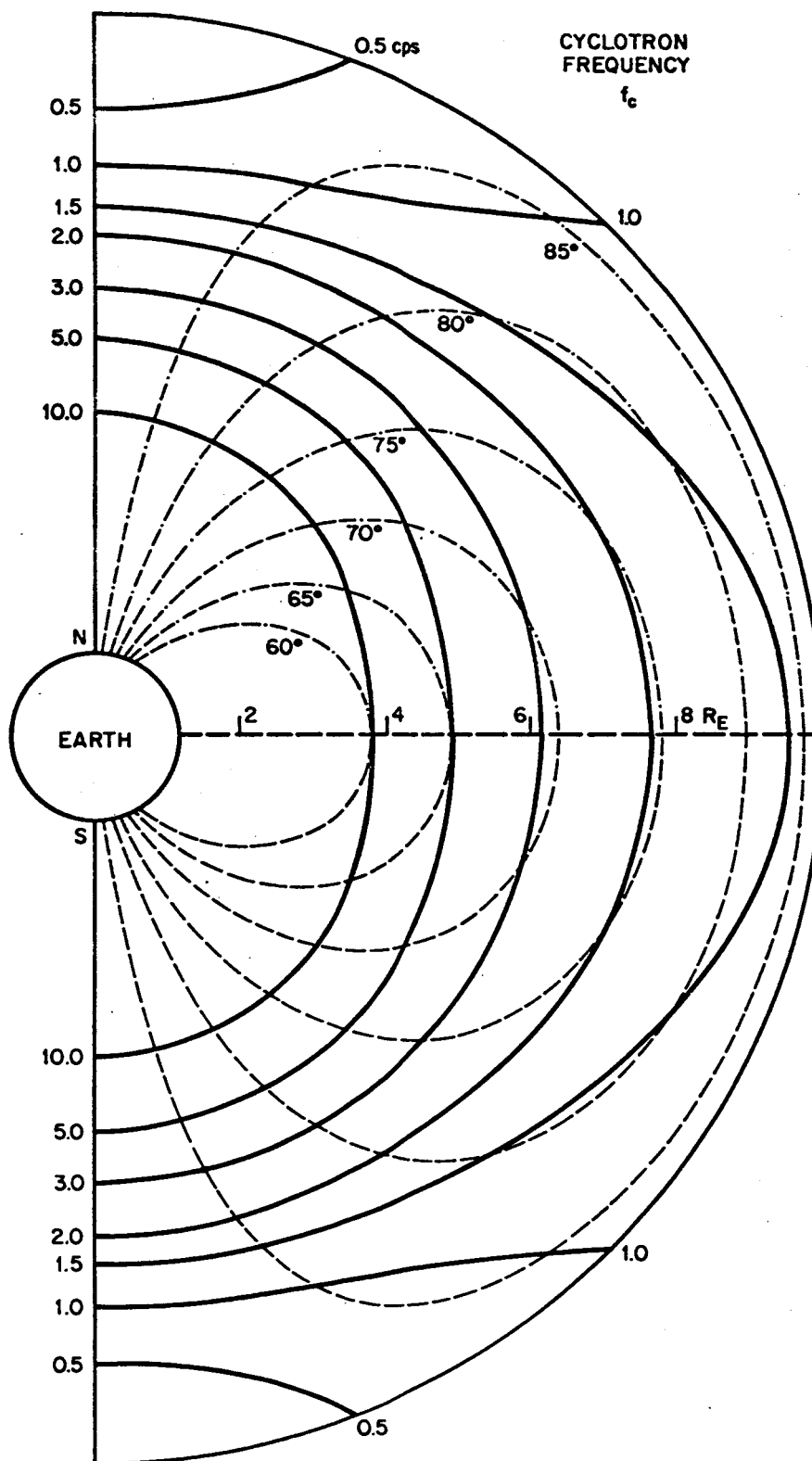


Figure 4. Proton cyclotron frequency contours for the dipole plus uniform field in the magnetosphere. Equal increments in earth radii are indicated by dots along the dipole plus uniform field (dashed lines).

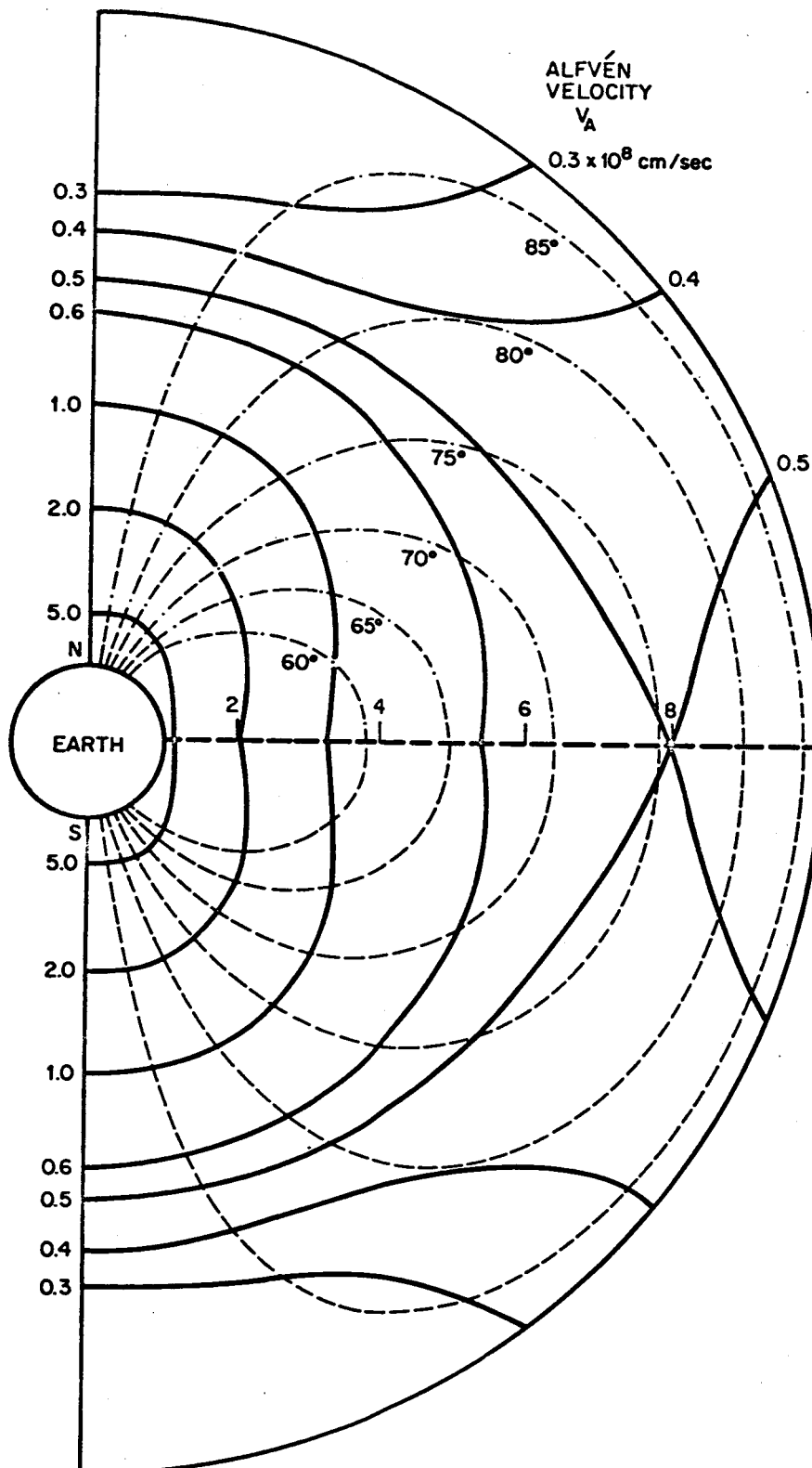


Figure 5. Alfvén velocity contours for the dipole plus uniform field and the Liemohn and Scarf (1964) inverse  $r$  cubed plasma density in the magnetosphere. The dipole plus uniform field is indicated by the dashed lines.

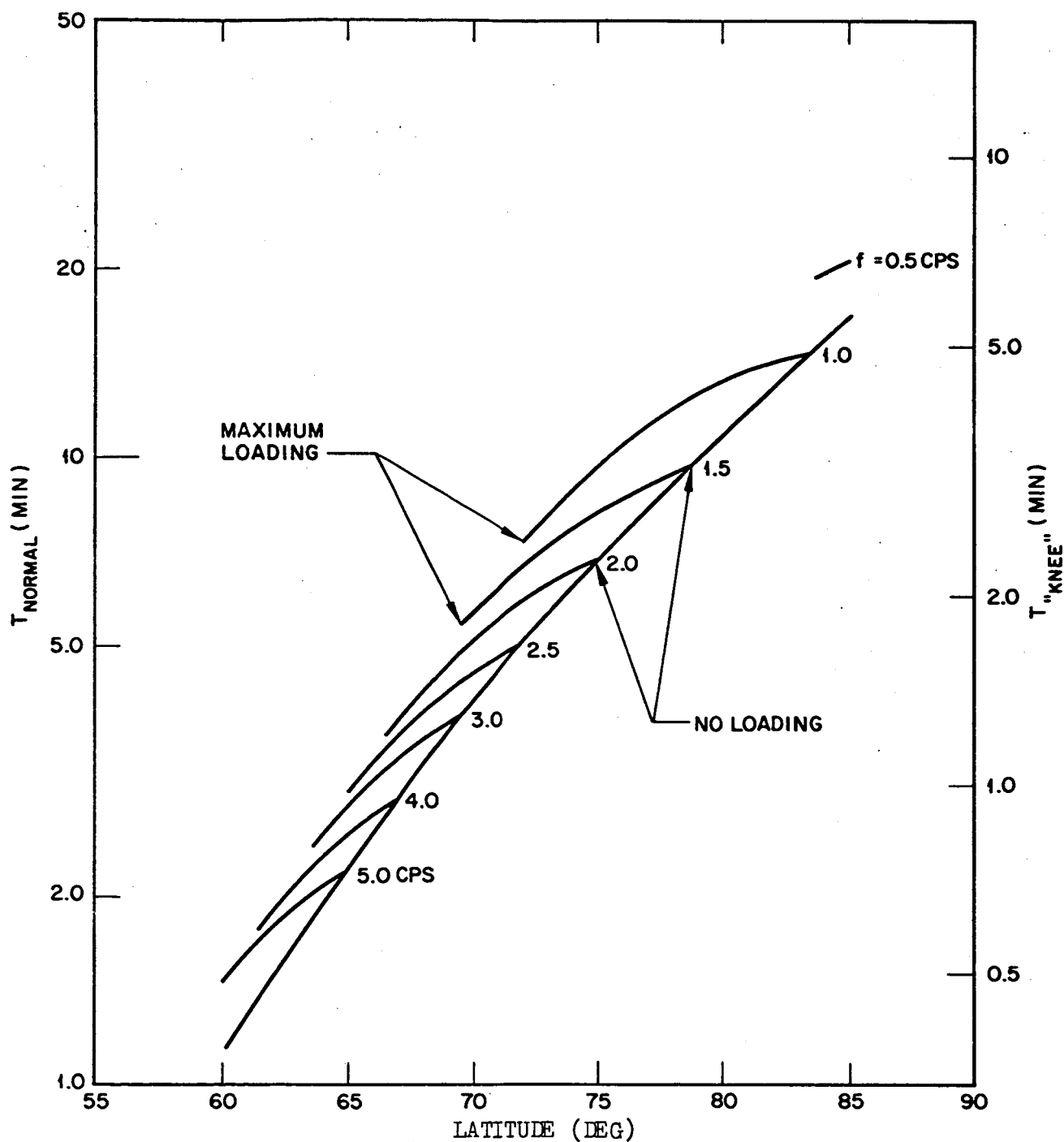


Figure 6. Alfvén wave bounce periods for the dipole plus uniform field and normal and "knee" plasma densities in the magnetosphere. The effect of diamagnetic loading of the field lines by ring current protons is included.

the component of stream velocity parallel to the magnetic field, designated by  $v_{\parallel}$ , can easily be calculated.

Let us consider in more detail the relative velocities of a hydromagnetic wave packet and proton stream characterized by the same bounce time, moving in the same direction, and crossing the equatorial plane at the same time. Since the Alfvén velocity varies substantially as the packet moves along a field line, whereas the stream velocity remains almost constant (except near the mirror points), it is clear that the stream moves more slowly than the wave packet lower down in the magnetosphere, and more rapidly than the wave packet higher in the magnetosphere near the equatorial plane. Thus "faster than light" motion occurs in extended regions in the vicinity of the equatorial plane. It is in these regions that the proton cyclotron radiation is subject to the anomalous Doppler shift and is likely to be most intense (Ginzburg, 1962).

The radiated frequency  $x = \omega/\omega_c$  is determined from Equation (4) after having calculated the proton velocity  $v_{\parallel}$  and the Alfvén velocity  $V_a$  in the manner just described. In this preliminary paper we restrict ourselves to the calculation of the radiated frequency only at the equatorial plane. However, it is clear from Figures 4 and 5 that there are extended regions on either side of the equatorial plane where both the proton cyclotron frequency and Alfvén velocity vary extremely slowly over large distances along a given magnetic field-line, so that almost the same frequency will be radiated over a large region.

The details of the calculations are given in later sections. We remark here that the results in best agreement with experimental observation were obtained when magnetospheric parameters were used which correspond to conditions of a "knee" in the plasma density (Carpenter, 1963) and a depression in magnetic field strength by a factor of about 2 (condition of maximum loading) at the equatorial plane where the emissions are generated. The latter condition seems quite reasonable in view of space probe measurements by Sonett et al (1960) and Smith (1962). In this regard, it may be significant that hm emissions have been found to be generated preferentially from 2 to 8 days after the sudden commencement of a magnetic storm (Wentworth, 1964a,c), a

time period in which an enhanced ring-current and a corresponding depression in the magnetic field is most likely to exist (E. J. Smith, private communication).

D. Explanation of rising-frequency fine structure. Perhaps the most striking single characteristic of most hm-emission bands is the rapidly-rising frequency of the fine-structured elements (Tepley, 1962; Tepley and Wentworth, 1962). In successive structural elements the higher frequencies sometimes tend to lag farther behind the lower frequencies (Figure 1). Jacobs and Watanabe (1964) have explained this effect in terms of dispersion of an Alfvén wave packet bouncing between hemispheres and closely guided by the geomagnetic field. Dispersion is introduced in the group velocity when the wave frequency approaches the local proton cyclotron frequency which can occur when the packet is relatively far out in the magnetosphere near the equatorial plane.

An alternative explanation may be offered in terms of the present model wherein the rising-frequency fine-structure and dispersion may be attributed to an initial velocity spread in  $v_{||}$ , the proton velocity component along the magnetic field line. According to the anomalous Doppler effect (Equations 4 and 5), relatively lower emission frequencies are generated by the faster particles in the stream, and conversely. Since the bounce time is shorter for the faster particles, the lower frequencies in successive fine-structured elements will be more closely spaced - hence, dispersion.

A numerical example is now presented to illustrate this effect. Consider the broad-band hm emission presented in Figure 1 (the same event was considered by Jacobs and Watanabe, 1964, to illustrate their dispersion calculation). In Table 1 are given the emission frequencies and fine structure repetition periods for corresponding parts of the emission band.

Let us assume that a relatively large anomalous Doppler shift occurs so that Equation (5) is valid, that is

$$\frac{f}{f_c} \approx \frac{V_a}{v_{||}}$$

Table 1. The hydromagnetic-emission event  
of November 2, 1961 observed at Palo Alto,  
California, and shown in Figure 1.

<u>Part of band</u>	<u>Emission Frequency f (cps)</u>	<u>Fine-structure Repetition period T (minutes)</u>
Upper: $f_1$	1.2	1.4
Center: $f_2$	1.5	1.7
Lower: $f_3$	1.8	2.0



It is to be noted that  $V_a$  does not actually represent the velocity of the hydromagnetic wave packet but is only a parameter resulting from considerations discussed previously (the wave packet propagates at the Alfvén mode group velocity which differs slightly from  $V_a$ ). We now specify that the fine-structure repetition period equals the bounce time of the proton stream which in turn is inversely proportional to the proton velocity  $v_{||}$ . We consider a proton stream with a velocity spread and associate the 3 selected emission frequencies with the corresponding values of proton velocity and bounce period. Thus

$$f_1 : f_2 : f_3 = T_1 : T_2 : T_3$$

Taking  $T_2 = 1.7$  minutes as the reference bounce time and substituting the tabulated values of  $f_1, f_2, f_3$  we calculate

$$\begin{aligned} T_1 &= 1.36 \text{ minutes} \\ T_3 &= 2.04 \text{ minutes} \end{aligned}$$

Comparing the calculated and measured values of bounce time we find a percentage deviation from the mean of 3% and 2% respectively.

It is interesting to note that the proton velocity dispersion mechanism considered above and the wave velocity dispersion mechanism considered by Jacobs and Watanabe (1964) may occur simultaneously when the frequency shift produced by the anomalous Doppler effect is relatively small. The combination of the two effects results in a tendency toward phase stability for particles and waves of different velocities. For example, the slower particles in the stream radiate the relatively higher frequencies closer to the local proton cyclotron frequency. Since these frequencies propagate more slowly in the region near the equatorial plane, the bounce time of the higher frequency portion of the wave packet will be relatively long corresponding to the relatively longer bounce time of the slower component of the stream. Conversely, the faster particles in the stream radiate relatively lower frequencies farther from the local cyclotron frequency. The lower frequencies propagate more rapidly at a group velocity which approaches the Alfvén velocity as the Doppler shift increases. Thus, the lower frequencies of the

wave packet and the faster protons which generate these frequencies both tend toward relatively short bounce times.

E. Latitude dependence of hydromagnetic-emission frequency. The earlier proton bunch model of Jacobs and Watanabe (1963) associates the hm-emission frequency with a hydromagnetic resonance effect in the lower exosphere. The model predicts an increase of emission frequency with increasing latitude. Experimentally, the opposite is observed (Tepley, 1964; Tepley et al, 1964; Wentworth, 1964a,b). The present model is in agreement with observation.

The observed emission frequency is a function of both the proton cyclotron frequency in the region where the signal is generated (presumably near the equatorial plane) and the ratio of stream-to-Alfven velocity which determines the extent to which the proton cyclotron frequency is lowered by the anomalous Doppler shift. The latter quantity is capable of wide variation and may be responsible for the bandwidth of the emission and the rising-frequency fine structure as considered previously. The proton cyclotron frequency, however, is dependent only on the spatial coordinates of the magnetic field and the extent to which the field is "loaded". In general the proton cyclotron frequency near the equatorial plane will decrease with increasing distance from the earth. Thus emissions generated at greater distances from the earth will be characterized by lower frequencies and will be guided by the magnetic field to the earth at higher latitudes. Thus the model predicts an inverse frequency-latitude dependence in agreement with observation.

F. Guidance of the hydromagnetic-wave packet. As demonstrated by Booker and Dyce (1963) and Jacobs and Watanabe (1964), the group velocity vector for the Alfven wave tends to propagate in the direction of the geomagnetic field. The actual extent of the guidance, however, is a function of the ratio of wave frequency to local proton cyclotron frequency, and varies with position as the packet moves along the field line. A quantitative investigation of the degree of guidance which occurs is likely to be quite difficult. The present model does not require extremely good guidance as does the 2nd model of Jacobs and Watanabe (1964) because energy is being

added to the wave packet each time it crosses the equatorial plane. However, several mechanisms for guidance are inherent in the model. These mechanisms may reinforce the natural tendency for Alfvén-wave guidance along the geomagnetic field. The guidance mechanisms are as follows:

(1) A natural duct is provided by the "loaded" magnetic field discussed in Part 3 of this report. It should be pointed out, however, that strong thermal and cyclotron (collisionless) hydromagnetic wave absorption may also occur in this duct since field loading is presumably produced by relatively energetic particles which may move at velocities comparable to the velocity of the hydromagnetic Alfvén wave packet. We have not yet investigated the relative importance of guidance and absorption in the loaded magnetic field ducts.

(2) A hydromagnetic "whispering gallery" is formed when an ion density "knee" exists in the magnetosphere. Thus emissions generated at latitudes below the knee will be reflected internally and thus guided along the field line which defines the position of the knee. This mechanism may significantly contribute to guidance of the Alfvén wave and will also produce guidance of the magneto-sonic wave also radiated by proton streams but which we do not consider further in this paper.

### III. ENERGY CONSIDERATIONS

A. Coherency of radiation. The concept of anomalously Doppler shifted cyclotron radiation from a single particle spiralling in a magneto-plasma is relatively easy to understand. The concept of radiation from a particle stream, however, is far more difficult to visualize since it depends on a collective interaction between particles in the stream and plasma. It is reasonable that the collective interaction should result in some degree of coherency in the motion of the stream particles and thus in coherent cyclotron radiation. The mathematically more rigorous treatments of related problems generally lead to formulas for the growth rate of the cyclotron "instability" as energy is transferred from the stream to the plasma (Stepanov and Kitsenko, 1961). Under certain conditions the growth rate is found to be quite rapid, a result which perhaps implies coherency of radiation.

In this section we assume coherency and present an order of magnitude calculation to demonstrate that cyclotron radiation from a reasonable number of protons is adequate to produce the observed hm emission magnetic field strength at the earth's surface. The calculation is based on the assumption that all of the radiating particles are collected into a single coherent cluster. It should be made clear that this assumption is made only to simplify the calculation, and is not meant to imply that such coherent clusters exist in the magnetosphere. It is also assumed for simplicity that in order of magnitude the total radiated energy is the same as that which would be radiated in an isotropic plasma where the magnitude of refractive index is the same as for the magneto-active plasma,  $N = C/V_\phi$ .

B. Energy radiated by a single proton. For a single proton spiraling in an isotropic plasma, the total energy radiated is given by

$$W_P = \frac{2}{3} \frac{e^2}{c^3} \omega_c^2 v_\perp^2 N x^2 \quad (6)$$

where  $e$  is the proton charge,  $c$  is the velocity of light,  $N$  is the refractive index of the plasma,  $\omega_c$  is the proton cyclotron frequency, and  $v_\perp = R\omega_c$  is the component of proton velocity perpendicular to its direction of motion ( $R$  is the proton gyro-radius). We neglect the radiation associated with the velocity component  $v_\parallel$  since this is Cerenkov Radiation which exhibits no preferential frequency dependence and is likely to be much lower in amplitude than cyclotron radiation (Ginzburg, 1962). We may also write

$$v_\perp^2 = \frac{2E}{M} \sin^2 \alpha \quad (7)$$

where  $E$  is the proton kinetic energy,  $M$  is the proton mass and  $\alpha$  is the pitch angle.

We take  $\alpha = 7^\circ$  (corresponding to a mirror point fairly low in the exosphere). For other numerical quantities we take values obtained from the solution of Figure 7 which predicts a 1.5 cps hm emission at a latitude of  $61^\circ$  radiated in a "normal" plasma and a "fully loaded" magnetosphere.

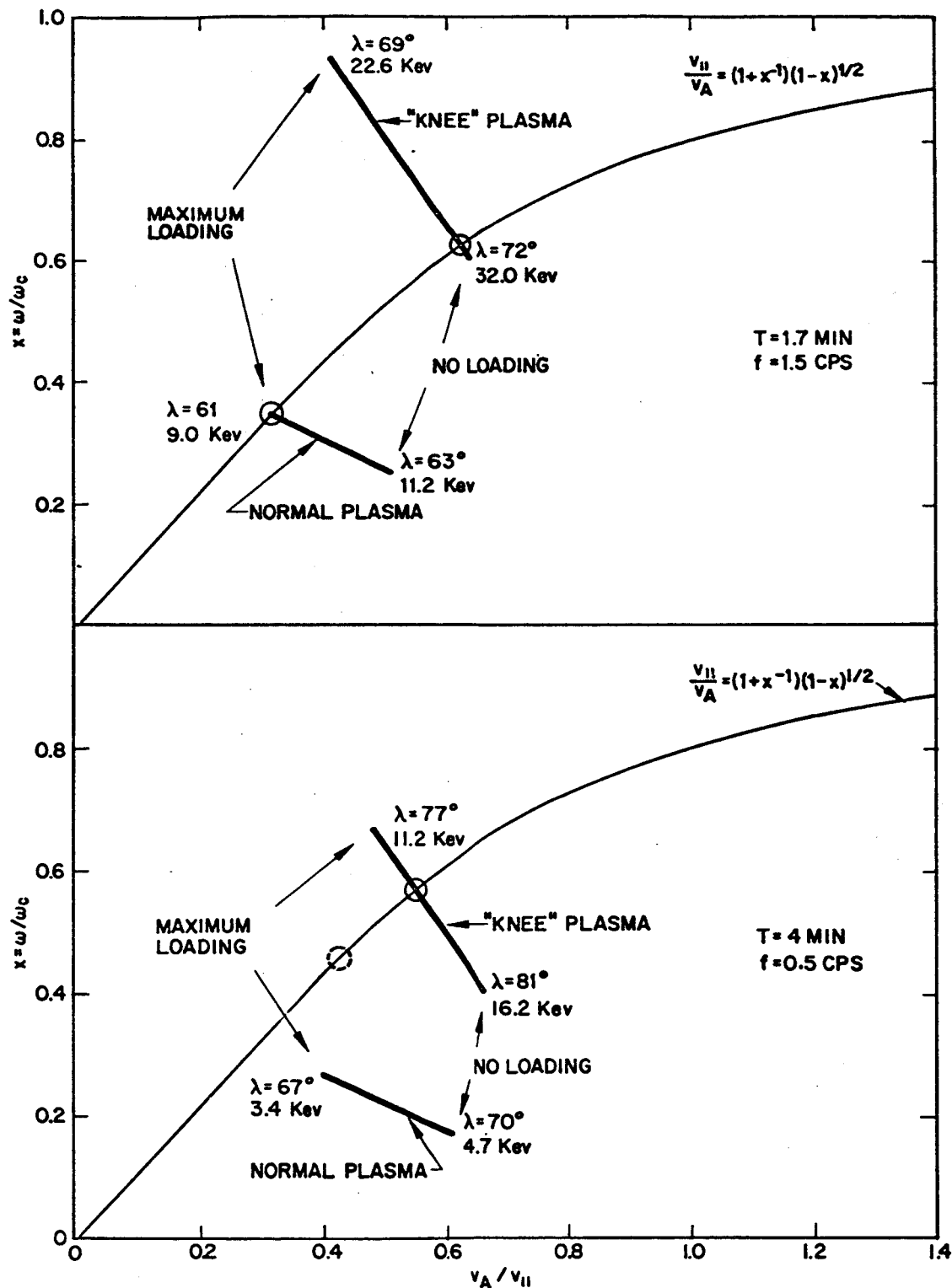


Figure 7. Self-consistent solutions for the proton cyclotron excitation model for the production of hydromagnetic emissions. The self-consistent solutions must lie along the continuous curve for  $x(V_a/v)$ .

The numerical values are:

$$\begin{aligned} E &= 9 \text{ kev} \\ N &\approx 1100 \\ \omega_c &\approx 28 \text{ radians/second} \\ x &\approx 0.34 \end{aligned}$$

Substituting into Equation (6) we obtain for the energy radiated for a single proton

$$W_p \approx 3(10^{-32}) \text{ ergs/sec}$$

C. Energy received at the earth's surface. Let us take  $\Delta B = 50$  milligauss =  $5(10^{-7})$  gauss which represents an extremely large hm emission. Since the signal is predominantly a magnetic disturbance, the corresponding energy density is  $(\Delta B)^2/8\pi \approx 10^{-14}$  ergs/cm<sup>3</sup>. Assuming that the energy density received at the earth's surface is the same as that which emerges from the ionosphere at the Alfvén velocity  $V_a = 2(10^7)$  cm/sec, then the power density at the earth's surface is  $2(10^{-7})$  erg/cm<sup>2</sup> sec.

D. Dimensions of the radiating proton stream. To the writers knowledge the anomalously Doppler shifted radiation pattern from a proton spiraling in a magneto-plasma has not yet been calculated. In order to calculate a lower limit to the number of protons required, we assume that all the radiation is perfectly guided in a tube of magnetic flux and focused toward the earth's surface. Let "A" be the area of the tube at the equatorial plane at 4 earth radii ( $\lambda \approx 61^\circ$ ) and "a" be its area at the surface of the earth. Since magnetic flux is conserved in the tube the ratio of energy density at the earth's surface to the energy density at the equatorial plane in the fully loaded magnetosphere is  $A/a \approx 200$ .

Assuming that the magnetosphere is loaded only by 9 kev protons, the proton density is found to be about  $40/\text{cm}^3$  at the equatorial plane. Let us assume that 10 percent of these protons are radiating coherently, so that the density of coherent particles is

$$n_p = 4 \text{ protons/cm}^3$$

We define the diameter of the stream to be the diameter of the flux tube, so that  $d = (4A/\pi)^{1/2}$ . We now make the extreme assumption that the length of

the stream is equal to its diameter, so that the stream particles are collected into a cluster. The number of protons in the cluster is then given by  $n_p dA$  and the energy radiated coherently is

$$W_{\text{radiated}} = (n_p dA)^2 W_p \quad (8)$$

The energy received at the earth's surface is  $2(10^{-7})a$ . Equating the energy radiated to the energy received and solving for the diameter of the cylinder we find

$$d = \left( \frac{8(10^{-7})}{\pi} \cdot \frac{1}{n_p^2 W_p} \cdot \frac{a}{A} \right)^{1/4} = 2.3(10^5) \text{ cm} \quad (9)$$

For the radiation to be fully coherent it is necessary that the cluster dimensions be much less than the wavelength of the radiated signal. The wavelength is given by

$$\lambda = \frac{V_\phi}{f} = \frac{c}{fN}$$

For  $N = 1100$  and  $f = 1.5$  cps, we obtain  $\lambda = 2(10^7)$  cm; thus  $\lambda/d \approx 100$ , so that the hypothetical cluster would radiate coherently as specified.

In the more realistic situation of a radiating stream, the length of the stream is likely to be much greater than the length of the hydromagnetic wave. Thus the degree of coherency of radiation would probably be far less than that resulting from a single proton cluster, but this would be at least partially compensated by the great increase in the number of radiating protons.

It is also of interest to calculate the proton gyro-radius given by

$$R = \frac{v_\perp}{\omega_c} = \frac{\sqrt{2E/M}}{\omega_c} \sin \alpha$$

For  $\alpha = 7^\circ$ ,  $\omega_c = 28$  and  $E = 9$  kev, we find  $R = 6(10^5)$  cm. Hence  $\lambda/R \approx 30$ . Thus the wavelength is much greater than the gyro-radius of any radiating proton in the stream.

#### IV. PARTICLE-WAVE MOTION IN THE MAGNETOSPHERE

In order to discuss the dynamics of particle and wave motion in the magnetosphere we need to establish models of the magnetic field and thermal plasma. We are then able to calculate properties of proton motion in the magnetosphere as well as Alfvén wave bounce periods along lines of force. Finally, we are able to show that self-consistent solutions for the model of hm-emission production exist.

A. The magnetic field of the earth. The magnetic field of the earth is normally taken to be that of a pure dipole at the center of the earth with magnetic moment  $M = 8.1 \times 10^{25}$  gauss-cm<sup>3</sup>. In the case of the real earth the magnetic field does not extend to infinity, but is cut off by the solar wind which limits it to an asymmetrical cavity, approximately hemispherical on the sun side, and having an average distance of approximately 10 earth radii from the center of the earth during geomagnetically quiet times. The effect of this cavity is approximately to add a uniform vertical magnetic field to the dipole magnetic field of the earth inside the cavity.

A uniformly magnetized sphere has a pure dipole field outside and a uniform field in its interior. Therefore, a dipole field can be limited to a spherical region of space by surrounding it with a spherical shell of surface currents which exactly cancel the dipole field outside the sphere and add a uniform field inside. The surface currents produced by the solar wind must therefore have approximately this effect in the case of the real earth, at least on the sun side.

If a uniform field  $B_0$  is added to the dipole magnetic field, the  $B_r$  and  $B_\lambda$  components become

$$\begin{aligned} B_r &= \left( -\frac{2M}{r^3} + B_0 \right) \sin \lambda \\ B_\lambda &= \left( \frac{M}{r^3} + B_0 \right) \cos \lambda \end{aligned} \tag{10}$$

and the equation of a line of force becomes

$$\cos^2 \lambda = \frac{r}{r_e} \frac{(1 - B_0 r_e^3 / 2M)}{(1 - B_0 r^3 / 2M)} \tag{11}$$



In our case, we set  $B_0 = 2M/(10R_E)^3 = 62.7$  gammas (1 gamma =  $10^{-5}$  gauss).

In Figure 3, the resultant field lines are compared with a model calculation of the deformation of the geomagnetic field by the solar wind (Mead, 1963). It can be seen that qualitatively the behavior of the field lines for the two models is similar, although quantitatively the Mead field lines lie closer to the cavity boundary. However, given the uncertainties in the initial conditions assumed in any model calculation, it is felt that a more detailed calculation than that based on the pure dipole plus uniform field is not justified at present.

B. Thermal plasma model in the magnetosphere. Two plasma models have been employed in the magnetosphere, the normal one falling off as  $r^{-3}$  (Liemohn and Scarf, 1964),

$$N_e = 1.41 \times 10^4 (R_E/r)^3 / \text{cm}^3 \quad (12)$$

and the "knee" model of Carpenter (1963) having the same  $r^{-3}$  dependence but lower in density by a factor of 9.

C. Charged particle motion in the magnetosphere. The characteristics of charged particle motion in a dipole plus uniform magnetic field in the magnetosphere are discussed by Wentworth and Tepley (1962). In particular, the total spiral arc length of a charged particle mirroring just above the surface of the earth is required in order to relate the bounce period of trapped protons to their velocities and energies. These quantities are tabulated for a number of different field lines in Table 2.

D. Alfven wave bounce periods. The Alfven wave velocity is given by

$$V_a = B / \sqrt{4\pi M N_e} \quad (13)$$

The above models of magnetic field and ion plasma density enable us to compute Alfven wave velocities in the magnetosphere. Contours of equal Alfven velocity are thus plotted in Figure 5 assuming the normal plasma density in Equation (12). It is then a simple matter to integrate the Alfven wave travel time along a line of force and obtain the Alfven wave bounce times plotted in Figure 6 (lower continuous curve running from  $60^\circ$  to  $85^\circ$ ). It should be noted here that the hydromagnetic wave packet propagates at the

Table 2. Parameters of proton motion in the Magnetosphere. The dipole plus uniform field is assumed with a cavity boundary at  $10 R_E$ . In addition the assumption is made that the protons reflect near the surface of the earth (see Wentworth and Tepley, 1962, for a general discussion of this calculation).

Geomagnetic Latitude $\lambda$	45	60	70	80	85	degrees
Total Spiral Arc Length ( $4S_c$ )	5.7	12.6	22.6	40.1	49.9	$\times 10^9$ cm
Proton Velocity for 4 min	0.24	0.52	0.94	1.67	2.08	$\times 10^8 \frac{\text{cm}}{\text{sec}}$
Bounce period of: 2 min	0.47	1.05	1.89	3.34	4.16	
Proton energy for 4 min	0.29	1.42	4.65	14.5	22.4	kev
Bounce period of: 2 min	1.16	5.70	18.6	58.0	89.7	
Proton drift rate 4 min	0.22	1.65	6.28	13.7	17.2	$\frac{\text{deg}}{\text{hour}}$
for bounce period: 2 min	0.87	6.63	25.1	54.7	68.9	

Alfven wave group velocity rather than the Alfven velocity. The two velocities may differ significantly when the wave packet is in the vicinity of the equatorial plane. Hence the calculated Alfven wave bounce times only approximate the wave packet bounce times. A more exact calculation is contemplated at a later date.

Let us now consider the effect of diamagnetic loading of the magnetic field lines. Suppose that a hot plasma of high energy protons is trapped in a flux tube along a line of force. If the energy density of the trapped protons approaches the energy density of the magnetic field, the resultant magnetic field in the flux tube is significantly lowered. In fact, it has been shown in Part 3 of this report that maximum loading of a field line results in the magnetic field strength being reduced to  $1/2$  of its original value, and the energy density of trapped protons which produces this effect is equal to  $1/4$  of the original magnetic field energy density. Thus the energy density of trapped protons is equal to the energy density of the perturbed field, and no additional particles can be contained by the perturbed field.

We now wish to calculate the Alfven wave bounce periods along loaded field lines where the amount of loading is chosen to produce a predetermined equatorial proton cyclotron frequency (Note in Figure 4 that for lines of force above  $80^\circ$  the minimum proton cyclotron frequency occurs off the equatorial plane; for those field lines the minimum proton cyclotron frequency instead of the equatorial value is implied in the following discussion). As an example let us assume that we desire an equatorial proton cyclotron frequency of 2 cps. We note from Figure 4 that the unloaded  $75^\circ$  field line is characterized by this value, while the unloaded  $67^\circ$  field line is characterized by a proton cyclotron frequency of 4 cps. Hence by fully loading the  $67^\circ$  field line, we obtain the same equatorial proton cyclotron frequency which characterizes the unloaded  $75^\circ$  field line. Therefore, the Alfven bounce period curve corresponding to an equatorial proton cyclotron frequency of 2 cps, runs between  $67^\circ$  for a fully loaded field and  $75^\circ$  for an unloaded field. From Figure 6 we see that with a normal thermal plasma, the Alfven bounce time is 6.8 minutes along the unloaded  $75^\circ$  field line, and 3.6 minutes

along the fully loaded  $67^\circ$  field line. Also the Alfvén bounce time along the unloaded  $67^\circ$  field line is 2.7 minutes.

In the case of the "knee" plasma density the above Alfvén bounce times are reduced by a factor of 3, becoming 2.3 minutes, 1.2 minutes, and 0.9 minutes respectively. In performing these calculations it has been assumed that the thermal plasma density along a loaded field line is unchanged from its unloaded value, and that the energy density of the hot trapped energetic protons is constant along the field line.

E. Self-consistent model calculations. The present model for the production of hm emissions has a number of parameters which must be self-consistent. As an example, consider an hm emission characterized by a fine structure repetition period of 4 minutes, and by a center frequency of 0.5 cps. Let us specify that the hydromagnetic wave packet is propagating in a plasma characterized by a density "knee". From Figure 6, the 4 minute Alfvén bounce period can occur between latitudes of  $77^\circ$  for a fully loaded field line and  $81^\circ$  for an unloaded field line. The 4 minute bounce time also specifies the energies of the protons bouncing in phase with the hydromagnetic wave packet as being between 11.2 kev at  $77^\circ$  and 16.2 kev at  $81^\circ$ . Finally, the frequency radiated by these protons as they pass through the equatorial plane with greater than Alfvén wave velocities is given approximately by Equation (5) for the anomalous Doppler effect.

This relation must hold for our example. Therefore, the self-consistent solution involving  $x = \omega/\omega_c$  determined by the observed emission frequency of 0.5 cps, the loaded equatorial proton cyclotron frequency between  $77^\circ$  and  $81^\circ$ , and the ratio  $v_{||}/V_a$  in the vicinity of the equatorial plane must lie on the above curve determined by Equation (5). In Figure 7,  $x$  has been plotted as a function of  $V_a/v_{||}$ . For the case of the "knee" density an intersection with the curve of Equation (5) exists at approximately  $x = 0.57$ . It is interesting to note that no intersection occurs for the above conditions for the normal plasma density. Therefore, since hm emissions having bounce periods of 4 minutes and frequencies of 0.5 cps are frequently observed at high latitudes, either "knee"-type plasma densities must occasionally exist in the magnetosphere, or the present model does not apply.

In a second case considered, corresponding to the hm emission shown in Figure 1 and discussed in an earlier section, the emission band center frequency is 1.5 cps and the corresponding bounce period is 1.7 minutes. Intersections for a self-consistent solution occur for normal plasma density at about  $61^{\circ}$  and for "knee" density at about  $72^{\circ}$ .

#### ACKNOWLEDGEMENTS

This work was conducted under contract NAS 5-3656 for the National Aeronautics and Space Administration. We wish to acknowledge Dr's. F. S. Johnson, S. F. Singer, M. Walt and W. Vali for stimulating and useful discussions.

## REFERENCES

- Booker, H. G. and R. B. Dyce, "Dispersion of waves in a cold magneto-plasma from hydrodynamic to Whistler frequencies", Stanford Research Institute report, August, 1963.
- Carpenter, D. L., "Whistler evidence of a 'knee' in the magnetospheric ionization density profile", J. Geophys. Research 68, 1675-1682, 1963.
- Gallet, R. M., "The very low-frequency emissions generated in the earth's exosphere", Proc. IRE 47, 211-231, 1959.
- Gallet, R. M. and R. A. Helliwell, "Origin of 'very-low-frequency emissions'", J. Res. NBS 63D (1), 21-27, 1959.
- Ginzburg, M. A., "A new mechanism producing short-period variations of the geomagnetic field", Bulletin of Academy of Sciences USSR, Geophysics Series, English Translation, 1096-1102, February 1962.
- Jacobs, J. A. and T. Watanabe, "Trapped particles as the origin of short period geomagnetic micropulsations", Planetary and Space Sciences 11, 869-878, 1963.
- Jacobs, J. A. and T. Watanabe, "Micropulsation whistlers", to be published in J. Atmospheric Terrest. Phys., 1964.
- Liemohn, H. B. and F. L. Scarf, "Whistler determination of electron energy and density distributions in the magnetosphere", J. Geophys. Research 69, 883-904, 1964.
- Mead, G. D., "The deformation of the geomagnetic field by the solar wind", NASA report X-640-63-246, submitted for publication to J. Geophys. Research (November, 1963).
- Sonett, C. P., E. J. Smith, D. L. Judge, and P. J. Coleman, Jr., "Current systems in the vestigial geomagnetic field: Explorer VI", Phys. Rev. Letters 4, 161-163, 1960.
- Smith, E. J., "A comparison of Explorer 6 and Explorer 10 magnetometer data", J. Geophys. Research 67, 2045-2049, 1962.
- Stepanov, K. N. and A. B. Kitsenko, "Excitation of electromagnetic waves in a magneto-active plasma by a beam of charged particles", Soviet Physics - Technical Physics, English Translation 6, 120-126, 1961.

- Tepley, L. R., "A study of hydromagnetic emissions", Sci. Rept. 2 (contract AF 19(604)-5906, Electronic Research Directorate, Air Research and Development Command), April 14, 1961a.
- Tepley, L. R., "Observations of hydromagnetic emissions", J. Geophys. Research 66, 1651-1658, 1961b.
- Tepley, L. R., "Structure and attenuation of hydromagnetic emissions", Vol. 1, Sci. Rept. 1 (contract AF 19(604)-5906, Electronic Research Directorate, Air Research and Development Command), April 6, 1962.
- Tepley, L. R., "Low-latitude observations of fine-structured hydromagnetic emissions", to be published in J. Geophys. Research 69, June 1, 1964.
- Tepley, L. R. and R. C. Wentworth, "Hydromagnetic emissions, X-ray bursts, and electron bunches, Part 1: Experimental results", J. Geophys. Research 67, 3317-3333, 1962.
- Tepley, L. R., R. C. Wentworth, and K. D. Amundsen, "Sub ELF geomagnetic fluctuations, Vol. I: frequency-time characteristics of hydromagnetic emissions", Final Report, contract AF 19(628)-462 for Air Force Cambridge Research Laboratory, Office of Aerospace Research, 26 December 1963.
- Wentworth, R. C., "Sub ELF geomagnetic fluctuations, Vol. II: statistical studies of hydromagnetic emissions", Final Report, contract AF 19(628)-462 for Air Force Cambridge Research Laboratory, Office of Aerospace Research, 26 December 1963.
- Wentworth, R. C., "Enhancement of hydromagnetic emissions following geomagnetic storms", to be published in J. Geophys. Research 69, June 1, 1964a.
- Wentworth, R. C., "Evidence for maximum production of hydromagnetic emissions above the afternoon hemisphere of the earth, Part I: Extrapolation to the base of the exosphere", to be published in J. Geophys. Research 69, July 1, 1964b.
- Wentworth, R. C., "Evidence for maximum production of hydromagnetic emissions above the afternoon hemisphere of the earth, Part II: Analysis of statistical studies", to be published in J. Geophys. Research 69, July 1, 1964c.
- Wentworth, R. C. and L. R. Tepley, "Hydromagnetic emissions, X-ray bursts, and electron bunches, Part II: Theoretical interpretation", J. Geophys. Research 67, 3335-3343, 1962.